# Photochemistry of HNCO in Solid Xe: Channels of UV Photolysis and Creation of $H_2NCO$ Radicals

**Mika Pettersson,* Leonid Khriachtchev, Santtu Jolkkonen, and Markku Räsänen**

*Laboratory of Physical Chemistry, P.O. Box 55, FIN-00014 University of Helsinki, Finland*

*Received: June 29, 1999; In Final Form: September 9, 1999*

Photolysis of HNCO at wavelengths between 266 and 193 nm is studied in solid Xe with FTIR and laser-induced fluorescence methods. The channels HNCO → H + NCO (a) and HNCO → NH + CO (b) are operative in a Xe matrix. Channel b produces both isolated fragments and NH···CO complexes as characterized by the CO absorption. The MP2/6-311++G(3df,3pd) calculations are presented for the NH−CO complexes and compared with the experimental data. Photolysis of NCO produces mainly NO + C. A part of the carbon atoms form $C_2$ after which $C_2^-$ is created in a photoinduced charge transfer reaction. For comparison, in solid Kr, photolysis of HNCO produces additionally HOCN but this channel is absent in a Xe matrix. Upon annealing of the partially photolyzed matrix at 50 K, hydrogen atoms are mobilized and a radical $H_2NCO$ is formed by a reaction of a hydrogen atom with a HNCO molecule. Four IR absorptions of $H_2NCO$ are observed and they agree well with the MP2/6-311++G(3df,3pd) calculations. The assignment is supported by experiments with DNCO. The threshold for the photodecomposition of $H_2NCO$ is between 365 and 405 nm.

## 1. Introduction

Photodissociation dynamics of HNCO has recently been a subject of intensive experimental and theoretical investigations.[1−7] A reason for the popularity of isocyanic acid in this context is that it can provide insight into processes connected with the photodissociation of a polyatomic molecule. These processes include competition of different reaction channels, intramolecular conversion (IC), intersystem crossing (ISC), and predissociation.

In the gas phase, HNCO can dissociate via the following chemical channels:

$$\mathrm{HNCO} \rightarrow \mathrm{NH}\,(\mathrm{X}^3\Sigma^-) + \mathrm{CO}\,(\mathrm{X}^1\Sigma^+) \quad D_0 = 30\,060\ \mathrm{cm}^{-1} \tag{1}$$

$$\rightarrow \mathrm{H}\,(^2\mathrm{S}) + \mathrm{NCO}\,(\mathrm{X}^2\Pi) \quad D_0 = 38\,370\ \mathrm{cm}^{-1} \tag{2}$$

$$\rightarrow \mathrm{NH}\,(\mathrm{a}^1\Delta) + \mathrm{CO}\,(\mathrm{X}^1\Sigma^+) \quad D_0 = 42\,750\ \mathrm{cm}^{-1} \tag{3}$$

The experimental values for the threshold energies are from ref 7 for (1) and (3) and from ref 2 for (2). The first allowed electronic transition $S_1 \leftarrow S_0$ of HNCO has an onset around 280 nm and extends to about 200 nm where the onset of another electronic transition is observed.[8,9] Channel 1 is open in this whole region and, according to Zyrianov et al., this channel is reached via the $S_1 \rightarrow S_0 \rightarrow T_1$ sequence.[7] Under photolysis below 260 nm, channel 2 becomes open and the quantum yield of NCO is about 1 around 235 nm.[10] Below 230 nm, channel 3 becomes dominant. According to ab initio calculations,[5] there is a barrier of more than 8000 $cm^{-1}$ on the $S_1$ surface for channel 2 and therefore this reaction proceeds via IC to $S_0$ and the dissociation takes place at the ground state. The barrier for channel 3 is only about 500 $cm^{-1}$.[7]

Photolysis of molecules in the condensed phase differs from that in the gas phase due to cage effect.[11−13] The cage effect prevents photofragments from being separated and leads to a reduced quantum yield for permanent photodissociation. In the matrix-isolation technique, the cage effect can be used to trap molecular complexes obtained in photodissociation of polyatomic molecules.[14,15] Some light atoms such as hydrogen show a high cage exit probability, especially in solid Xe.[12] After permanent separation of the photofragments, thermal mobilization of them can be used to synthesize novel compounds.[16]

Jacox and Milligan photolyzed HNCO in an Ar matrix and found that UV irradiation with a medium pressure mercury lamp mainly forms HOCN and the amount of HN + CO is very small.[17] NCO was not observed, indicating that in solid Ar cage exit for hydrogen atom is not probable upon photolysis at around 250 nm. When the same authors used VUV radiation at 121.6 nm, the formation of NCO was observed,[18] and this can be understood by the enhanced cage exit probability of hydrogen atom with the larger excess energy. Maas et al. photolyzed HNCO in an Ar matrix by a bromine lamp which emits radiation in the 150−165 nm range, and they obtained both isolated NH and NH···CO complex as evidenced by laser-induced fluorescence (LIF).[19]

In this paper, we report the results of photolysis of HNCO in Xe matrices. For comparison, a number of experiments were performed in Kr matrices. FTIR and LIF methods are combined to obtain reliable information on different photolysis products and processes. It is shown that the photochemistry of HNCO in solid Xe differs a lot from that in solid Ar or Kr and reasons for this difference are discussed. In annealing of the partially photolyzed matrix, the H + HNCO reaction produces a radical $H_2NCO$ which is directly observed for the first time.

## 2. Experimental Details

The matrices were made by depositing the premixed gas onto a CsI substrate. For HNCO, the matrix ratio of 1:2000 and deposition temperature of 30 K for Xe and 20 K for Kr produced highly monomeric matrices. For NO/Xe = 1:2000 mixture, the

* Corresponding author. E-mail: petters@csc.fi.

10.1021/jp992224d CCC: $18.00 
Published on Web 10/23/1999

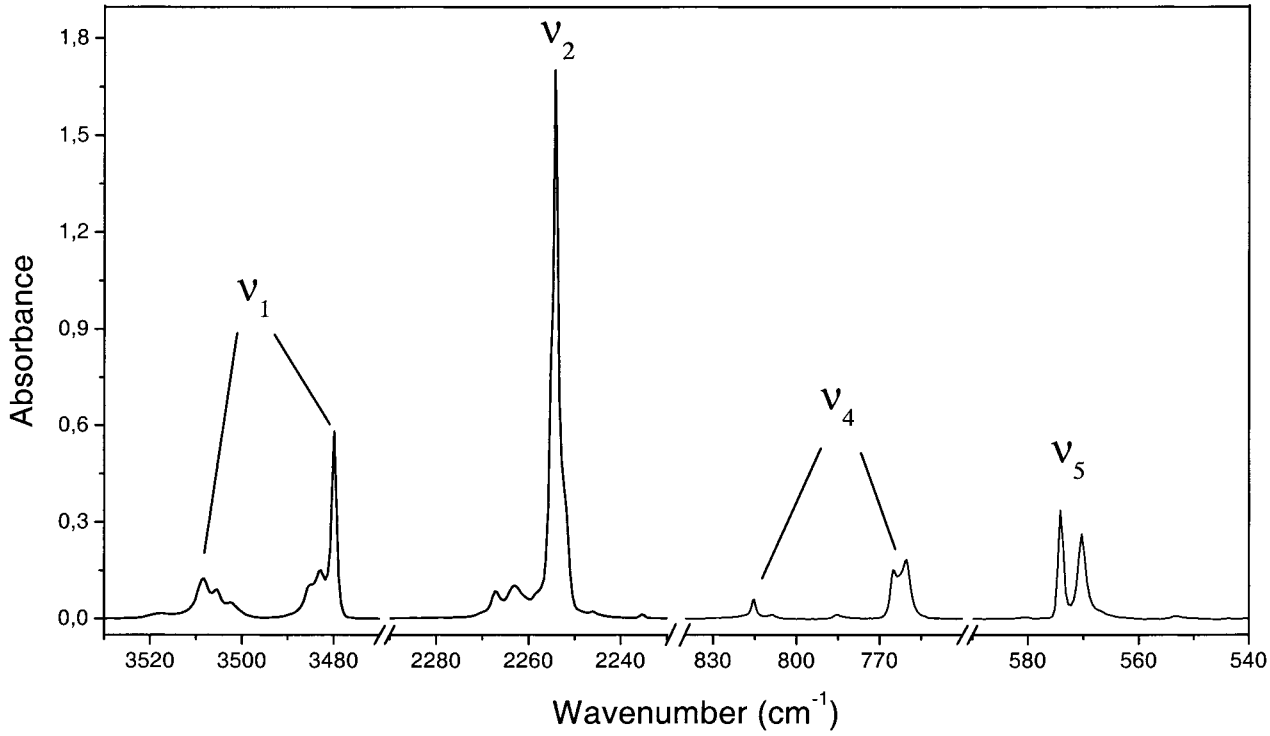


**Figure 1.** IR spectrum of a HNCO/Xe = 1:2000 matrix at 17 K. The sample was deposited at 30 K.

deposition temperature of 30 K yielded mostly $(NO)_2$ but the deposition temperature of 20 K provided a highly monomeric matrix. After deposition, the samples were cooled to 7.5 K and the photolysis was carried out at this temperature.

HNCO was synthesized from cyanuric acid (Merck, 99.5%) vaporized at 350 C°. The vapor was transferred along with a carrier gas (nitrogen) to an owen held at 750 C°. At this temperature, cyanuric acid decomposed to HNCO, which was trapped by a −100 C° bath and purified by low temperature and pressure distillation. DNCO was prepared by recrystallizing HNCO from $D_2O$ several times, and the vacuum and deposition lines were passivated with $D_2O$. We obtained matrices with more than 50% of DNCO as evidenced by the IR spectrum. Rare gases (99.997%, AGA) and NO (99.5%, Messer Griesheim) were used without further purification.

HNCO was photolyzed by an excimer laser (ELI 76, Estonian Academy of Sciences) operating at 193 nm with pulse energy of about 20 mJ and pulse duration of 10 ns. Photolysis at longer wavelengths as well as excitation of photoproducts was carried out by the fourth harmonic (266 nm) of a Nd:YAG laser (Continuum, Powerlite) or doubled radiation of an optical parametric oscillator (OPO, Sunlite with FX-1, Continuum), with pulse duration of ∼5 ns and pulse energy of ∼10 mJ. The pulse energies were measured by a laser power meter (MAX 5200, Molectron). The IR spectra were recorded by a Nicolet 60 SX spectrometer with resolution of 1 or 0.25 $cm^{-1}$. The emission spectra were measured with a single UV−visible spectrometer (Spex 270 M, resolution 0.3 nm) equipped with a gated ICCD camera (Princeton Instruments).

## 3. Computational Details

The calculations were carried out with the Gaussian 98 package[20] using a second-order perturbation theory (MP2). Structures of the molecular species were fully optimized and the harmonic wavenumbers were obtained at the MP2/6-311++G(3df,3pd) level of theory. The NH−CO complex interaction energies were evaluated by calculating the monomer energies in the dimer-centered basis set which yielded BSSE-corrected values. The computations were carried out on SGI Origin 2000 computers at the CSC, Center for Scientific Computing Ltd. (Espoo, Finland).

**TABLE 1: IR Absorption Bands of HNCO in Xe and Kr Matrices**

| Kr ($cm^{-1}$) | Xe ($cm^{-1}$) | assignment[a] |
|---|---|---|
| 553.0 | 553.2 | $\nu_5(1\leftarrow1)$ |
| 571.3, 572.9 | 570.3, 574.2 | $\nu_5(0\leftarrow0)$, doublet |
| 695.6 | 694.7 | $\nu_6(1\leftarrow0)$ |
| 763.6 | 760.3, 765.1 | $\nu_4(0\leftarrow0)$, doublet |
| 787.0 | 785.6 | $\nu_4(1\leftarrow1)$ |
| 816.8 | 808.8, 815.5 | $\nu_4(1\leftarrow0)$, doublet |
| 2261.6 | 2254.4 | $\nu_2(0\leftarrow0)$ |
| 2255.8, 2261.6, 2269.5, 2272.3 | 2258.8, 2263.0, 2267.3, 2270.5 | $\nu_2$ sidebands |
| 3496.9 (shoulder), 3500.6 | 3479.9, 3483.0, 3485.2 | $\nu_1(0\leftarrow0)$ |
| 3509.4 (shoulder), 3514.7 | | $\nu_1(0\leftarrow0)$[b] |
| 3529.6 | 3502.3, 3505.5, 3508.4 | $\nu_1(1\leftarrow0)$ |

[a] Assignment follows ref 22. The numbers in parentheses indicate $K_a$ quantum numbers. [b] In the Kr matrix $\nu_1$ $(0\leftarrow0)$ is split by a Fermi-type resonance in analogy to the Ar matrix (see ref 22).

## 4. Results

**4.1. FTIR Observations.** Since the IR absorption spectrum of HNCO is known in Ar, Ne, and $N_2$ matrices,[17,21,22] it is of interest to report the spectrum in Kr and Xe matrices as well. Figure 1 shows the IR spectrum of monomeric HNCO in solid Xe, and the positions of the absorptions of HNCO in Xe and Kr matrices are collected in Table 1.

Photolysis of HNCO in solid Xe was carried out at several wavelengths between 266 and 193 nm. Irrespective of the photolysis wavelength, monomeric CO appeared at 2132.8 $cm^{-1}$, and in addition, two slightly blueshifted bands at 2138.5 and 2144.4 $cm^{-1}$ were observed, indicating that complexed CO was formed (see Figure 2). A redshifted band at 2124.5 $cm^{-1}$

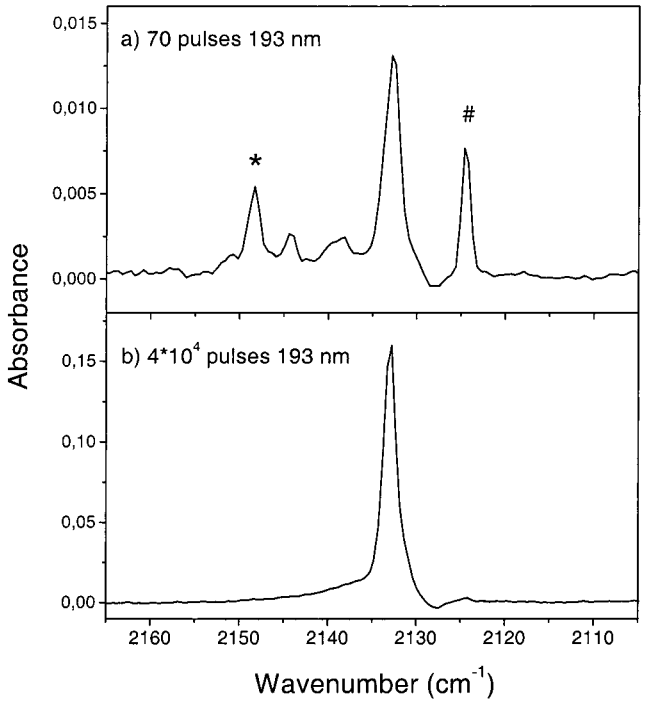


**Figure 2.** IR spectrum of CO produced by photolyzing HNCO with 193 nm in a Xe matrix. (a) presents the situation after 70 pulses showing the appearance of monomeric CO and NH···CO complexes and HXeNCO (marked with an asterisk) and probably $NCO^-$ (marked with "#"). (b) shows the situation after 40 000 pulses where only monomeric CO is present and CO complexes, HXeNCO, and $NCO^-$ have been photolyzed. The parts a and b are individually scaled.

appeared in photolysis, and the assignment of this band is discussed later. The growing band at 2148.3 $cm^{-1}$ does not belong to a CO complex but to HXeNCO molecule (see later). All the bands in this region except the CO monomer band reached maximum intensity at an early stage of the photolysis and decreased upon prolonged irradiation finally disappearing completely as shown in Figure 2.

A doublet at 1915.9 and 1917.8 $cm^{-1}$ grew fast in the beginning of the photolysis, achieved maximum intensity, and decreased slowly (see Figure 3). This doublet can be safely assigned to NCO radical on the basis of the known wavenumber in an Ar matrix[18] at 1933 $cm^{-1}$ from which the Xe value is shifted downward by ~17 $cm^{-1}$. We also observed bending absorption of NCO at 1269.0 $cm^{-1}$, which compares well with the corresponding band in an Ar matrix at 1275 $cm^{-1}$.[18]

During photolysis, another band at 1866.7 $cm^{-1}$ with a shoulder at 1864.8 $cm^{-1}$ appeared and grew monotonically approaching saturation in the long photolysis. Figure 3 demonstrates an intermediate situation when both NCO and the new band are well visible. The band at 1866.7 $cm^{-1}$ was assigned to NO, and the assignment was proved by preparing a NO/Xe = 1:2000 matrix that gave the monomeric NO band exactly at the same position. The shoulder band did not appear in the as-deposited matrices, and we tentatively assign this band to another site of NO produced only in the photolysis or to a NO···C complex.

We did not observe any absorptions around 1800 $cm^{-1}$ which could be assigned to a CNO radical.[23] No sign of HOCN or other isomers such as HCNO or HONC was found either. NH was not observed in the IR measurements possibly because the absorption is very weak.[18] Finally, $Xe_2H^+$ appeared in photolysis, indicating that ionic channels were also available.[24] All the observed IR bands appearing in the photolysis of HNCO in solid Xe are collected in Table 2.

In solid Kr, two main photolysis products were observed, HOCN and both monomeric and complexed CO, which was evidenced by growth of three bands at 2135.4 (monomer), 2140.0, and 2141.7 $cm^{-1}$ (complexed). HOCN was identified by using the bands at 3536.6, 2291.1, 1220.6, and 1088.6 $cm^{-1}$ which are near the corresponding values in Ar matrices.[17,22] Photolysis at 193 nm caused NCO radical to appear at 1921.6 $cm^{-1}$, but the band was much weaker than in Xe matrices, indicating that NCO is a minor product in a Kr matrix.

**4.2. LIF Observations.** Although NH was not observed in IR measurements, the strong CO bands appearing upon photolysis indicate that NH should be formed as well. Indeed, the emission of NH was observed when excited at 338.5 nm corresponding to the $A^3\Pi \leftarrow X^3\Sigma^-$ transition.[19] Both $b^1\Sigma^+ \rightarrow X^3\Sigma^-$ and $a^1\Delta \rightarrow X^3\Sigma^-$ emissions were detected as presented

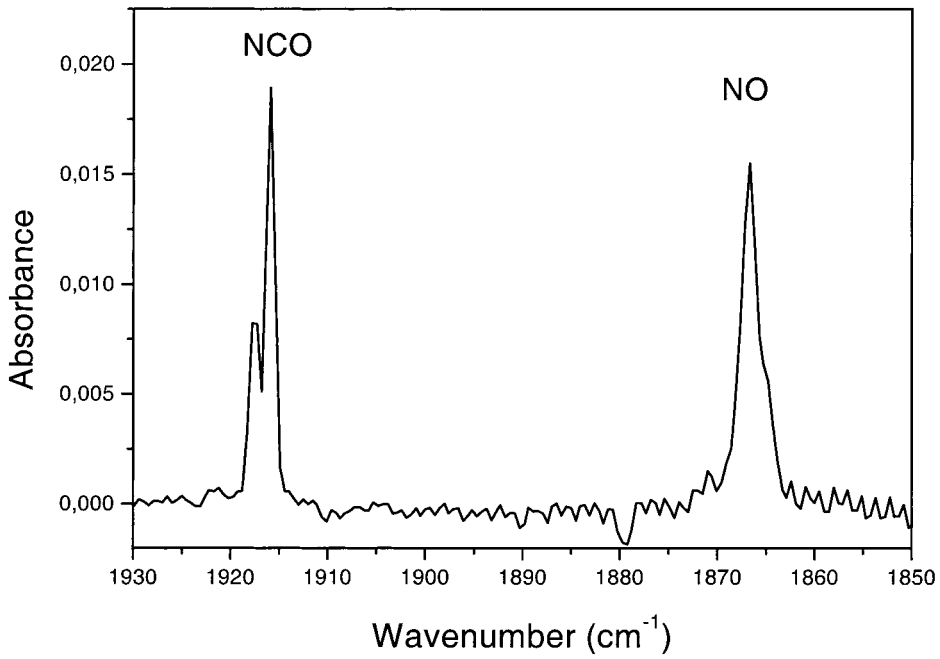


**Figure 3.** IR spectrum of NCO and NO appearing after irradiating a HNCO/Xe = 1:2000 sample with 10 000 pulses of the ArF laser (193 nm).

**TABLE 2: Bands Appearing in Photolysis of HNCO in Solid Xe and after Annealing of the Photolyzed Matrix**

| wavenumber ($cm^{-1}$) | appearance (p = photolysis, a = annealing) | assignment |
|---|---|---|
| 1076.5 | a | HCO $\nu_2$ |
| 1166, 1181 | a | $XeH_2$ |
| 1214.4 | a | $H_2NCO$ |
| 1269.0 | p | NCO $\nu_2$ |
| 1555.8 | a | $H_2NCO$ |
| 1623.8 | a | HXeCN |
| 1731.0 | a | $HCONH_2$ |
| 1788.1, 1793.2 | p, a | HXeNCO |
| 1794.2, 1796.6, 1806.5, 1811.8 | a | $H_2NCO$ |
| 1851.0 | a | HXeNC |
| 1856.6, 1858.4 | a | HCO $\nu_1$ |
| 1864.8 | p | NO at site b, or a NO···C complex (tentative) |
| 1866.7 | p | NO |
| 1915.9, 1917.8 | p | NCO $\nu_3$ |
| 2124.5 | p | $NCO^-$ (tentative) |
| 2132.8 | p | CO (monomer) |
| 2138.5 | p | NH···CO complex |
| 2144.4 | p | NH···CO complex |
| 2148.3 | p, a | HXeNCO |
| 2442.3 | a | HCO $\nu_3$ |
| 3518.5 | a | $H_2NCO$ |
| 3802.1, 3805.8 | p | NCO $2\nu_3$ |

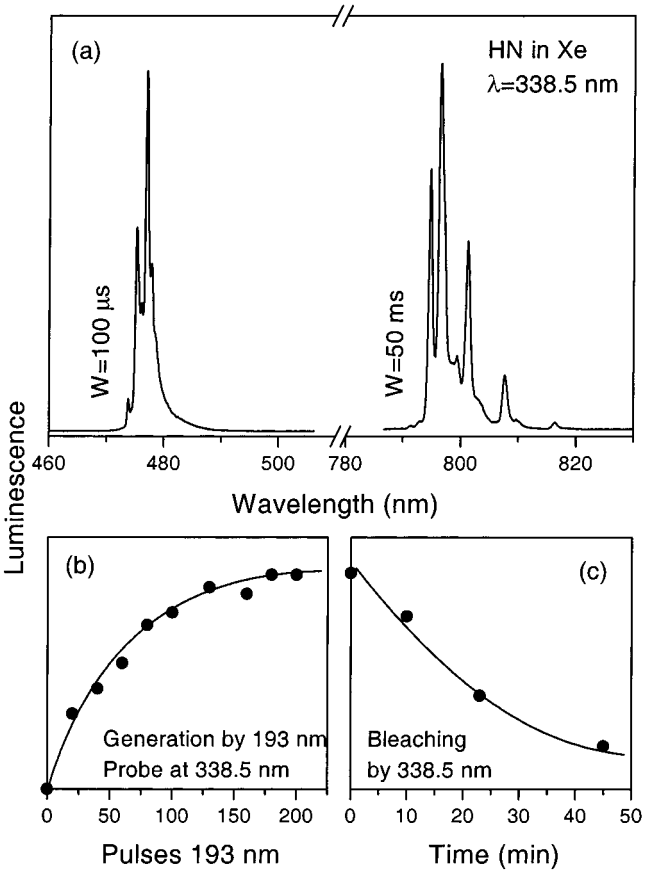


**Figure 4.** Luminescence spectrum of NH excited by the 338.5 nm radiation (a), the generation of the luminescence during 193 nm photolysis of HNCO (b), and its bleaching by resonant irradiation with 338.5 nm (c). The gate width (*W*) used is indicated in (a).

in Figure 4a. The emissions show well-resolved structures attributable to rotation of NH in accordance with refs 19 and 25. For $a^1\Delta \rightarrow X^3\Sigma^-$, transitions from the $J' = N' = 2$ level of the upper electronic state to the $N'' = 0, 1, 2, 3, 4$ levels of the

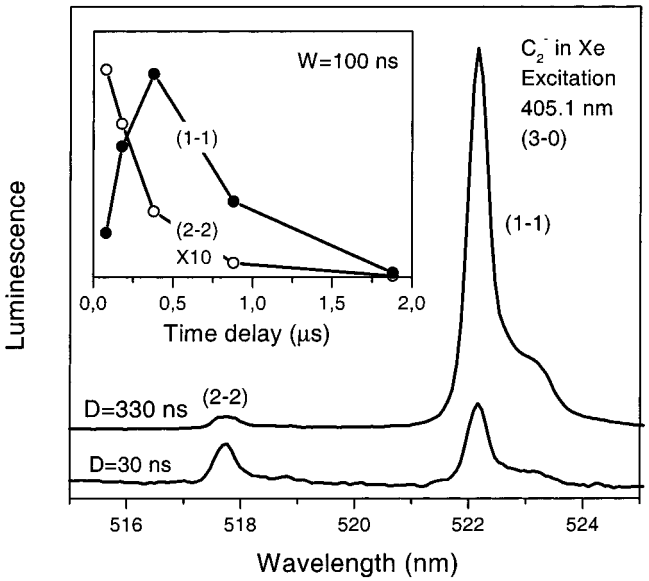


**Figure 5.** B → X luminescence spectrum of $C_2^-$ generated by 193 nm photolysis of HNCO in solid Xe. The excitation wavelength is 405.1 nm. The 1−1 and 2−2 emission bands are shown at two different delays (*D*). In the insert, the effect of the delay to the intensities of the two bands is shown.

lower electronic state are observed and a rotational constant of 16.8 $cm^{-1}$ for the ground-state NH is obtained. This value is equal to the gas-phase rotational constant of NH (16.7 $cm^{-1}$)[26] within our experimental accuracy, which indicates free rotation of NH in a Xe matrix. The emission of NH is generated in 193 nm photolysis, and upon irradiation at 338.5 nm the NH emission bleaches as shown in parts b and c of Figure 4. Irradiation at 338.5 nm also induces changes in the IR spectrum. The band at 2124.5 $cm^{-1}$ and $Xe_2H^+$ grow and NCO decreases. In addition, monomeric and complexed CO decrease by a small amount and HNCO increases.

The decomposition of NCO and the appearance of NO seen in the photolysis indicate that carbon atoms are formed. Unfortunately, our excitation wavelength region does not allow direct detection of the emission of carbon atoms. Nevertheless, evidence for the creation of carbon atoms is provided by the observation of the emission from $C_2^-$.[27] Figure 5 shows the B → X (2−2) and (1−1) emissions of $C_2^-$ which are excited by 405.1 nm corresponding to the B($\nu = 3$) ← X($\nu = 0$) transition of $C_2^-$. The emission spectrum is given for two different time delays presenting the effect of vibrational relaxation.[28] In the insert, the time dependence of these emissions are shown and our data is in agreement with ref 28. Since the matrix contains $C_2^-$ it must also contain neutral $C_2$, but we did not detect any luminescence which could be assigned to $C_2$.

Oxygen atoms were observed by exciting charge transfer between Xe and O at 240 nm and monitoring the emission at 370 and 750 nm.[29] The oxygen atom emission appeared even under 240 nm photolysis, which indicates that O atoms do not originate from impurity water. It was concluded that O atoms are generated from HNCO possibly via NCO that can be photolyzed to CN and O.[18] Thermally, O atoms disappeared when the matrix was warmed to 45 K. In addition, H atoms were detected by LIF via 193 nm induced emission around 250 nm,[30] and the $A^2\Sigma \rightarrow X^2\Pi$ emission of NO was detected upon excitation at 225 nm.[31,32]

Figure 6 presents the kinetics of product concentrations during 193 nm photolysis of a HNCO/Xe matrix. The curves were obtained from IR measurements by integrating proper absorption bands of the species in question or from the LIF intensity ($C_2^-$).

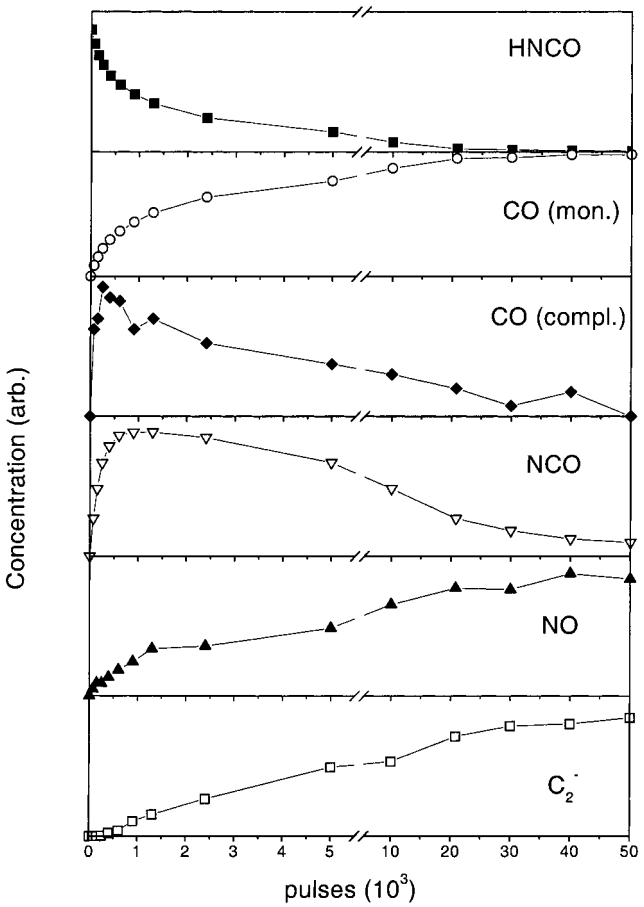


**Figure 6.** Kinetics of HNCO and of its photolysis products in the 193 nm photolysis. The concentrations were obtained by integrating relevant IR bands or from the luminescence intensity for $C_2^-$. Note the change of scale at 5500 pulses.

**4.3. Annealing.** When the photolyzed matrix is annealed at 50 K, a doublet band of $XeH_2$ appears at 1166 and 1180 $cm^{-1}$.[33] Bands growing at 2442.3, 1856.6, and 1076.5 $cm^{-1}$ are assigned to HCO by a comparison with the known IR spectrum in an Ar matrix.[34] During the annealing, monomeric CO decreases typically by 30−40%. In some experiments, a weak band at 2680.7 was observed and it might belong to HNO formed via the reaction H + NO → HNO.[35]

A number of bands around 1800 $cm^{-1}$ appear in annealing. If the photolysis is stopped when HNCO is mostly decomposed and NCO is abundant, a band at 1788.1 with a weaker component at 1793.2 $cm^{-1}$ is particularly prominent, and these bands correlate with a strong band at 2148.3 $cm^{-1}$. These bands belong to a novel rare gas compound HXeNCO but its characterization is a topic of another report.[36] In addition to HXeNCO, the weak absorptions of HXeCN and HXeNC molecules are found indicating that CN was present in small amounts in the matrix prior to annealing.[37]

One previously unknown set of bands appears upon annealing. When the matrix is annealed in the early stage of the photolysis when a significant proportion of HNCO is still present, a quartet at 1794.2, 1796.6, 1806.5, and 1811.8 $cm^{-1}$ is produced. Additionally, bands at 3518.5, 1555.8, and 1214.4 $cm^{-1}$ correlate with the quartet. These bands are shown in Figure 7. A band at 1731 $cm^{-1}$ is also prominent and it is known to belong to formamide ($HCONH_2$).[38] The remaining HNCO decreases typically by about 35% during annealing indicating reaction of HNCO. In experiments with DNCO, the absorptions around 1800 $cm^{-1}$ were slightly shifted and it was possible to resolve the bands at 1793.9, 1796.3, 1797.8, and 1800.2 $cm^{-1}$ although the absorptions of the H-form were also present. In addition, new weak absorptions were observed at 3503.8, 2634.4, and 1434.7 $cm^{-1}$, which are assigned to deuterated analogues of the new species.

Finally, different annealing products were separated by photodecomposition at different wavelengths. For example, 405 nm irradiation efficiently decomposed HXeNCO but did not decrease bands associated with the quartet around 1800 $cm^{-1}$. These bands can be destroyed with 365 nm radiation. The IR bands appearing upon annealing of the photolyzed HNCO/Xe matrices are collected in Table 2.

**4.4. Computational Results.** The calculated parameters are collected in Table 3 for NH−CO complexes and in Table 4 and Figure 8 for $H_2NCO$, HDNCO, and $D_2NCO$. The computational results are discussed in the next section in connection with the experimental results.

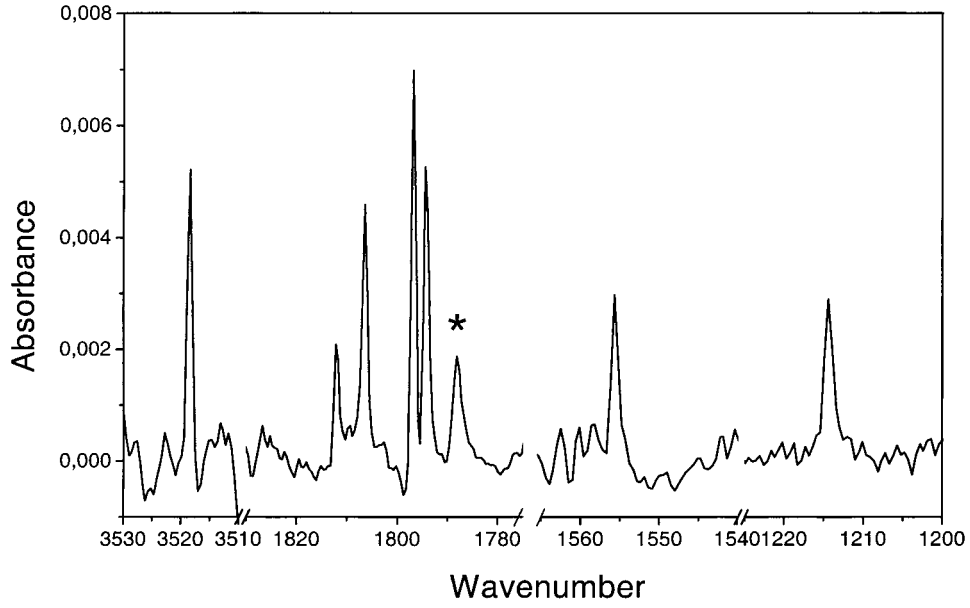


**Figure 7.** IR spectrum of $H_2NCO$ obtained by annealing at 50 K of the partially photolyzed HNCO/Xe = 1:2000 matrix. The spectrum is measured at 7.6 K. The band marked with an asterisk belongs to HXeNCO (see text for details).

**TABLE 3: MP2/6-311++G(3df, 3pd) Calculated Parameters of NH, CO, and the NH···CO and NH···OC Complexes**

| parameter | NH···CO | NH···OC | CO | NH |
|---|---|---|---|---|
| $r$(C−O) (Å) | 1.1344 | 1.1360 | 1.1355 | |
| $r$(N−H) (Å) | 1.0298 | 1.0298 | | 1.0300 |
| $r$(H−C)/$r$(H−O) (Å) | 2.6223 | 2.5152 | | |
| ∠(NHC)/∠(NHO) | 167.5° | 171.9° | | |
| ∠(HCO)/∠(HOC) | 172.2° | 173.8° | | |
| ∠(NHCO)/∠(NHOC) | 0.0° | 0.0° | | |
| $E$ (hartree) | −168.2573436 | −168.2563382 | −113.1367332 | |
| $E_{int}$(BSSE corrected) (cm$^{-1}$) | 348 | 140 | | −55.1183392 |
| $\nu_{CO}$ (cm$^{-1}$)[a] | 2139.2 (33) | 2128.4 (48) | 2131.2 (36) | |
| $\nu_{NH}$ (cm$^{-1}$)[a] | 3440.9 (<1) | 3444.0 (2) | | 3434.3 (12) |

[a] The values in parentheses are the calculated intensities in km/mol.

**TABLE 4: Calculated (MP2/6-311++G(3df,3pd)) and Experimental Bands of $H_2NCO$[a]**

| symmetry | calcd (cm$^{-1}$) $H_2NCO$ | obsd (cm$^{-1}$) $H_2NCO$ | calcd (cm$^{-1}$) HDNCO | calcd (cm$^{-1}$) $D_2NCO$ | obsd (cm$^{-1}$) HDNCO + $D_2NCO$ |
|---|---|---|---|---|---|
| A″ | 196.8 (207) | | 173.8 (147) | 152.5 (107) | |
| A′ | 535.7 (6) | | 486.5 (5) | 471.9 (4) | |
| A″ | 624.2 (0) | | 583.0 (8) | 508.3 (1) | |
| A′ | 1096.5 (1) | | 994.4 (4) | 914.1 (4) | |
| A′ | 1240.6 (69) | 1214.4 | 1180.6 (39) | 1097.6 (9) | |
| A′ | 1618.3 (55) | 1555.8 | 1488.8 (83) | 1303.4 (94) | 1434.7 (HDNCO) |
| A′ | 1884.6 (330) | 1794.2 | 1883.7 (321) | 1881.4 (327) | 1793.9 |
| | | 1796.6 | | | 1796.3 |
| | | 1806.5 | | | 1797.8 |
| | | 1811.8 | | | 1800.2 |
| A′ | 3581.9 (26) | | 2634.7 (20) | 2589.2 (31) | |
| A′ | 3776.4 (87) | 3518.5 | 3750.7 (86) | 2792.2 (44) | 3503.8 (HDNCO) |
| | | | | | 2634.4 ($D_2NCO$) |

[a] The numbers in parenthesis are the calculated intensities in km/mol.

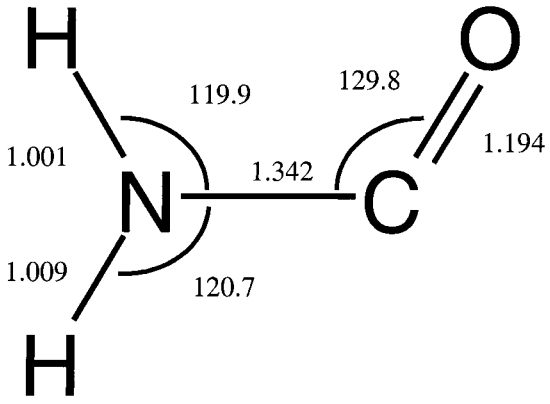


**Figure 8.** Structure of planar $H_2NCO$ calculated at the MP2/6-311++G(3df,3pd) level of theory.

## 5. Discussion

**5.1. HNCO and Its Photolysis.** The IR spectrum of HNCO in solid Kr and Xe shows that it rotates almost freely around one axis, similar to the case of solid Ar.[22] The analysis of the spectrum yields about 30 cm$^{-1}$ for the *A* rotational constant in solid Kr and Xe similarly to an Ar matrix.[22] The assignment of the bands is straightforward following ref 22 because the spectra in Kr and Xe matrices resemble closely the spectrum in an Ar matrix. The only noticed difference is that $\nu_1$ (0←0) is not split by a Fermi-type resonance in a Xe matrix as it is in Ar and Kr matrices.

The products of the photolysis of HNCO are strongly dependent on the solid host and the photolysis wavelength. In an Ar matrix, the main product in the photolysis with a mercury lamp was HOCN and the yield of CO was minor.[17] In solid Kr, the situation changes and both HOCN and CO are observed in large amounts while NCO can be produced only by 193 nm irradiation and even in this case its concentration is rather low. In addition, in an Ar matrix, NCO was observed when HNCO was photolyzed at 121.6 nm.[18] In solid Xe, the NCO bands become rather strong, indicating that channel 2 is effective presumably because hydrogen atom can escape from the parent cage. Additionally, CO is observed in large amounts but HOCN is not produced at all. These differences can be understood by the cage effect. For an Ar matrix, the effect is strong even for the hydrogen atom escape, and consequently, cage exit takes place only at very high excess energies. For solid Kr, the situation is somewhat intermediate and cage exit of H atoms is observed already at 193 nm. In solid Xe, hydrogen atom exit is more probable and NCO is formed in large quantities.

The yield of CO (and NH) can also be influenced by the cage exit probability of these fragments. In the gas phase, (NH + CO) pair can be formed by the channel 3 at the $S_1$ electronic state when the photolysis wavelength exceeds the threshold energy or by channel 1 via ISC.[7] The same behavior holds for solid environment as well, but in the matrix, the separation of the fragments is prevented by the cage effect. If the system is prepared at the $S_1$ state, it can reform HNCO after the fragments have collided with the cage walls. HNCO can be reformed via triplet state as well by the following mechanism. Because the $T_0$ state is bound with respect to the ground-state NH and CO,[39] the (NH + CO) pair can form a triplet molecule which can recover HNCO by ISC to $S_0$. Only if the (NH + CO) triplet pair relaxes to the complex form which is prevented to recombine by a potential barrier[39] of ∼1500 cm$^{-1}$ will the photoproduct be the NH−CO complex. In the case of cage exit, the products are isolated CO and NH. In long photolysis, the

complex is decomposed most probably via photolysis of NH or via regeneration of HNCO.

The appearance of the CO bands, which are shifted from the monomeric CO, indicates complexed CO. There are four possible configurations of NH−CO complexes, two of them corresponding to the hydrogen bonded NH···CO and NH···OC forms and the other two to the HN···CO and HN···OC forms. We studied these complexes by ab initio calculations, and only the hydrogen-bonded forms were found to be true minima on the multidimensional potential energy surface of this system. The structural and spectral properties of the two stable complexes are given in Table 3. The NH···CO form is the most stable complex with a BSSE-corrected interaction energy of 348 $cm^{-1}$. The important difference between the NH···CO and NH···OC is that the calculated shift for the CO stretch is upward and downward from the monomer, respectively, similarly to $H_2O$−CO complex in ref 40. The blue-shifted bands were observed both in Xe and Kr matrices, and they are assigned to NH···CO complex.

The red-shifted band was observed only in a Xe matrix, but the assignment of this band to NH···OC is problematic because there is no observable deuteration effect on this band although NH···CO bands are slightly but definitely shifted. This indicates that the species responsible for the 2124.5 $cm^{-1}$ band does not contain hydrogen. We suggest that this band belongs to $NCO^-$ and the assignment is based on several observations in addition to the absence of deuteration effect. The position of the band practically coincides with the gas-phase value of 2124.3 $cm^{-1}$ for $\nu_3$ of $NCO^-$.[41] $\nu_1$ and $\nu_2$ were observed at 1200.6 and 628.0 $cm^{-1}$ in solid KI,[42] but in our experiments they were not observed. However, according to theory,[43] $\nu_1$ is about a factor of 20 and $\nu_2$ a factor of 60 weaker than $\nu_3$, and they are presumably too weak to be observed in our experiments. Importantly, under 338.5 nm irradiation NCO absorption decreases, the 2124.5 $cm^{-1}$ band increases, and $Xe_2H^+$ increases as well. This indicates a charge-transfer process between NCO and Xe which produces $Xe_2H^+$ and the counterion $NCO^-$. The large electron affinity of NCO (3.6 eV)[44] favors such a process at relatively low photon energies such as in the case of $C_2$. On the basis of these considerations, we tentatively assign the 2124.5 $cm^{-1}$ band to $NCO^-$, but this assignment should be verified, for example, with experiments with isotopic substitution.

The 338.5 nm irradiation, which is resonant with NH, decreased slightly monomeric and complexed CO while simultaneously incresing HNCO. Conversion of the NH···CO complex to HNCO by excitation of NH is understandable. For the decrease of monomeric CO we suggest the following: isolated NH is excited which photomobilizes it or increases its reaction radius and it can react with a nearby CO molecule. It is probable that NH and CO are not separated extensively but form rather a close pair separated perhaps by one lattice constant. A similar situation occurs, for example, in photolysis of $H_2S_2$ where light-induced short-range mobility of the sulfur atoms is observed after photolysis.[45]

In the prolonged photolysis, NCO is decomposed to NO and C as evidenced by a rise of monomeric NO. In the 193 nm photolysis, this process is very slow compared to decomposition of the precursor as it can be seen in Figure 6. According to the calculations, the dissociation energy of NCO into $C(^3P)$ + $NO(^2\Pi)$ is 6.7 eV,[46] and it seems unlikely that the decomposition occurs in one step. Rather we suggest that NCO is first isomerized to CNO which is then photolyzed to C + NO. According to Persson et al., the latter process needs only 4.1 eV.[46] Another minor channel NCO → CN + O takes place which is evidenced by the observation of oxygen atoms by LIF and the formation of HXeCN and HXeNC in annealing. The amount of CN is too low to be detected by FTIR, and on the basis of our previous experiments[37] on HCN we estimate the upper limit of 10% for the yield of CN from HNCO. In addition to C + NO and CN + O channels, we cannot exclude the possibility of decomposition of NCO to CO + N which occurs in an Ar matrix.[18]

**SCHEME 1**

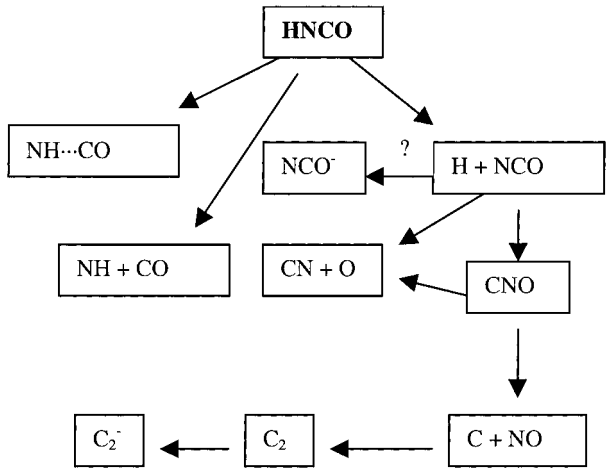


By a comparison of an extensively irradiated matrix, where most of HNCO is converted to CO and NO, with directly deposited NO/Xe and CO/Xe matrices we can estimate that roughly 70% of HNCO goes to CO and 30% of it forms NO when other channels are neglected. Since NCO can be converted mainly to NO + C, we must conclude that a large number of carbon atoms is created. Part of them recombine to $C_2$ and further UV irradiation can induce charge-transfer between Xe and $C_2$ and $C_2^-$ ions are formed. Permanent charge separation and trapping has been found especially in connection with halogen atoms in solid Xe.[47] The large electron affinity of $C_2$ (3.27 eV) brings the energetic threshold for the photon-induced charge-transfer down, and we can estimate in analogy with a bromine atom which has a similar electron affinity that the charge-transfer absorption should lie around 300 nm.[47] $C_2^-$ has been extensively studied in various rare gas matrices, and the identification of our emission is straightforward on the basis of the known spectroscopic constants.[27]

The results of the photolysis of HNCO in solid Xe are described qualitatively in Scheme 1. Altogether rather complete fragmentation of HNCO is observed in a prolonged photolysis and the stable photoproducts are CO, NO, CN, H, C, O, $C_2^-$, and presumably $C_2$. Intermediate photoproducts include NCO, HXeNCO, NH, HN−CO complexes, and probably CNO and $NCO^-$.

**5.2. Reactions of Mobile Hydrogen Atoms: $H_2NCO$ Radical.** There are several indications of reactions of hydrogen atoms upon annealing of the photolyzed matrix. Formation of HXeH, HCO, HXeCN, HXeNC, and HXeNCO[36] directly indicates the presence of hydrogen atoms.

An additional unknown product is evidenced by IR bands at 3518.5, ~1800 (quartet), 1555.8, and 1214.4 $cm^{-1}$. The formation temperature (~45 K) of this compound correlates with the global mobility of hydrogen atoms which prompts us to look for possible products formed from H atoms upon reaction with other species present in the matrix. The yield of the product is the largest when the matrix is warmed after short photolysis.

After long photolysis, the yield is very small, indicating that the new species does not correlate with NO, CO, or $C_2$. It does not correlate with NCO either because its maximum concentration occurs in annealing of the matrix before NCO reaches its maximum.

Formation of the new species correlates with the amount of unphotolyzed HNCO, and we consider the products of H + HNCO reaction. Actually, because the remaining concentration of HNCO decreases typically by about 35% when hydrogen atoms are mobilized, this reaction seems probable. Nguyen et al. have studied by ab initio calculations the H + HNCO → $H_2N$ + CO reaction and found two stable intermediates which can be formed in an exothermic reaction corresponding to the attachment of the hydrogen atom either to the oxygen or nitrogen of HNCO.[48] Formation of the oxygen bound form requires the activation energy of about 100 kJ/mol, and even its thermodynamical stability with respect to H + HNCO is questionable. Therefore, we neglect this product in our consideration. Formation of the other configuration has an activation barrier of about 40 kJ/mol, and when the possibility of tunneling and uncertainty in the computational results are taken into account, this reaction seems possible in our matrix environment at about 50 K.

The radical $H_2NCO$ shown in Figure 8 is a global minimum on the H + HNCO surface. Our calculated parameters are presented in the figure, and they do not differ much from the lower-level values of Nguyen et al.[48] According to the calculated spectrum (see Table 4), the four most intensive fundamentals are exactly in the regions where the absorptions of the new species are observed. For comparison, we have calculated the spectrum of HNCO at the same level of theory. According to those results, the asymmetric NH stretch of $H_2NCO$ is shifted by +47 $cm^{-1}$ from the corresponding HNCO value, and this is in a good agreement with the observed value of +39 $cm^{-1}$. Additionally, our most intensive band is a quartet at the 1800 $cm^{-1}$ region, and the same band is the strongest computationally.

The deuteration experiments support strongly the assignment of the new species to $H_2NCO$. For the strongest band, NCO stretch, our calculations predict a shift of −0.9 $cm^{-1}$ for HDNCO and −3.2 $cm^{-1}$ for $D_2NCO$. Experimentally, we observe several slightly shifted bands at 1793.9, 1796.3, 1797.8, and 1800.2 $cm^{-1}$. Although we cannot assign each band specifically to HDNCO or $D_2NCO$, the observed shifts are in a good agreement with the computational predictions. A new weak band at 3503.8 $cm^{-1}$ is safely assigned to the N−H stretch of HDNCO and the observed shift from the $H_2NCO$ band at 3518.5 $cm^{-1}$ is −14.7 $cm^{-1}$, in agreement with the calculated shift of −25.7 $cm^{-1}$. A band at 2634.4 $cm^{-1}$ is assigned to the N−D stretch of $D_2NCO$. One more band at 1434.7 $cm^{-1}$ is assigned to the HDNCO analogue of the 1555.8 $cm^{-1}$ band of $H_2NCO$, and the experimental shift of −121.1 $cm^{-1}$ agrees well with the computed shift of −129.5 $cm^{-1}$. Other bands of the deuterated forms are either too weak to be observed or overlapped with other absorptions.

Further support to the assignment is obtained by identifying a band at 1731 $cm^{-1}$ to formamide ($HCONH_2$). The formation of formamide indicates the reaction H + $H_2NCO$ → $HCONH_2$, and according to this $H_2NCO$ should be present in the matrix. In addition, the assignment of the new bands to $H_2NCO$ is supported by the photolysis experiments with formamide.[49] The bands assigned to $H_2NCO$ in the present work were found in the photolysis of formamide indicating the minor channel $HCONH_2$ → $H_2NCO$ + H.

On the basis of the facts presented above, we assign the new bands to $H_2NCO$. Currently, we do not have an explanation for the quartet structure of the ∼1800 $cm^{-1}$ band, but the constant ratio of the intensities of the four bands from experiment to experiment suggests that the splitting is due to intrinsic properties of the molecule rather than due to a site effect.

It is interesting to note the analogy to our previous experiments with HCN in solid Xe and Kr.[37] In those experiments, we obtained $H_2CN$ from HCN by photolyzing the precursor partially and mobilizing hydrogen atoms after photolysis in a reaction H + HCN → $H_2CN$. It appears that by controlled photolysis and annealing of Xe matrices doped with small hydrogen-containing molecules one can obtain interesting radical species in a convenient way.

## 6. Conclusions

Photochemistry of HNCO is studied in Xe matrices by FTIR and LIF methods. It is found that in the early stage main products are H atoms, NCO, HXeNCO, HN−CO complexes, and isolated CO and NH. Further photolysis leads to a decomposition of NCO mainly into carbon atoms and NO and to some extent into CN + O. Part of the carbon atoms move and recombine to form $C_2$, from which $C_2^-$ is formed by photoinduced charge transfer.

In annealing of the photolyzed Xe matrix, new species are formed upon a thermal mobilization of the isolated hydrogen atoms. $H_2NCO$ radical is formed from the remaining precursor HNCO by a reaction with a hydrogen atom. The IR spectrum of $H_2NCO$ is presented experimentally for the first time. The threshold for the photodecomposition of this radical lies between 365 and 405 nm. In addition, annealing leads to formation of HCO, HXeNCO, HXeCN, HXeNC, and HXeH.

**Acknowledgment.** M. P. thanks the Academy of Finland for the financial support. CSC-Center for Scientific Computing is appreciated for providing computer mainframe time. Henrik Kunttu is thanked for generously providing NO.

## References and Notes

(1) Zhang, J.; Dulligan, M.; Wittig, C. *J. Phys. Chem*. **1995**, *99*, 7446.
(2) Zyrianov, M.; Droz-Georget, Th.; Sanov, A.; Reisler, H. *J. Chem. Phys*. **1996**, *105*, 8111.
(3) Brown, S. S.; Cheatum, C. M.; Fitzwater, D. A.; Crim, F. F. *J. Chem. Phys*. **1996**, *105*, 10911.
(4) Zyrianov, M.; Droz-Georget, Th.; Reisler, H. *J. Chem. Phys*. **1997**, *106*, 7454.
(5) Klossika, J.-J.; Flöthmann, H.; Beck, C.; Schinke, R.; Yamashita, K. *Chem. Phys. Lett*. **1997**, *276*, 325.
(6) Stevens, J. E.; Cui, Q.; Morokuma, K. *J. Chem. Phys*. **1998**, *108*, 1452.
(7) Zyrianov, M.; Droz-Georget, Th.; Reisler, H. *J. Chem. Phys*. **1999**, *110*, 2059.
(8) Dixon, R. N.; Kirby, G. H. *Trans. Faraday Soc*. **1968**, *64*, 2002.
(9) Rabalais, J. W.; McDonald, J. R.; McGlynn, S. P. *J. Chem. Phys*. **1969**, *51*, 5103.
(10) Brown, S. S.; Metz, R. B.; Berghout, H. L.; Crim, F. F. *J. Chem. Phys*. **1996**, *105*, 6293.
(11) Bondybey, V. E.; Brus, L. E. *J. Chem. Phys*. **1975**, *62*, 620.
(12) Schriever, R.; Chergui, M.; Schwentner, N. *J. Phys. Chem*. **1991**, *95*, 6124.
(13) Gödderz, K. H.; Schwentner, N.; Chergui, M. *J. Chem. Phys*. **1996**, *105*, 451.
(14) Lundell, J.; Räsänen, M. *J. Phys. Chem. A* **1995**, *99*, 14301.
(15) Heikkilä, A.; Pettersson, M.; Lundell, J.; Khriachtchev, L.; Räsänen, M. *J. Phys. Chem. A* **1999**, *103*, 2945.
(16) Pettersson, M.; Lundell, J.; Räsänen, M. *Eur. J. Inorg. Chem*. **1999**, 729.
(17) Jacox, M. E.; Milligan, D. E. *J. Chem. Phys*. **1964**, *40*, 2457.
(18) Milligan, D. E.; Jacox, M. E. *J. Chem. Phys*. **1967**, *47*, 5157.
(19) Maas, M.; Gross, Ch.; Schurath, U. *Chem. Phys*. **1994**, *189*, 217.
(20) Frisch, M. J.; Trucks, G. W.; Schlegel, H. B.; Scuseria, G. E.; Robb, M. A.; Cheeseman, J. R.; Zakrzewski, V. G.; Montgomery, J. A., Jr.; Stratmann, R. E.; Burant, J. C.; Dapprich, S.; Millam, J. M.; Daniels, A. D.; Kudin, K. N.; Strain, M. C.; Farkas, O.; Tomasi, J.; Barone, V.; Cossi,

M.; Cammi, R.; Mennucci, B.; Pomelli, C.; Adamo, C.; Clifford, S.; Ochterski, J.; Petersson, G. A.; Ayala, P. Y.; Cui, Q.; Morokuma, K.; Malick, D. K.; Rabuck, A. D.; Raghavachari, K.; Foresman, J. B.; Cioslowski, J.; Ortiz, J. V.; Stefanov, B. B.; Liu, G.; Liashenko, A.; Piskorz, P.; Komaromi, I.; Gomperts, R.; Martin, R. L.; Fox, D. J.; Keith, T.; Al-Laham, M. A.; Peng, C. Y.; Nanayakkara, A.; Gonzalez, C.; Challacombe, M.; Gill, P. M. W.; Johnson, B.; Chen, W.; Wong, M. W.; Andres, J. L.; Gonzalez, C.; Head-Gordon, M.; Replogle, E. S.; Pople, J. A. *Gaussian 98*, revision A.3; Gaussian, Inc.: Pittsburgh, PA, 1998.

(21) Bondybey, V. E.; English, J. H.; Mathews, C. W.; Contolini, R. J. *J. Mol. Spectrosc*. **1982**, *92*, 431.

(22) Teles, J. H.; Maier, G.; Hess, B. A., Jr.; Schaad, L. J.; Winnewisser, M.; Winnewisser, B. P. *Chem. Ber*. **1989**, *122*, 753.

(23) Persson, B. J.; Roos, B. O.; Carter, S. *Mol. Phys*. **1995**, *84*, 619.

(24) Kunttu, H.; Seetula, J.; Räsänen, M.; Apkarian, V. A. *J. Chem. Phys*. **1992**, *96*, 5630.

(25) Blindauer, C., van Riesenbeck, N.; Seranski, K.; Winter, M.; Becker, A. C.; Schurath, U. *Chem. Phys*. **1991**, *150*, 93.

(26) Huber, K. B.; Herzberg, G. *Molecular Spectra and Molecular Structure, Vol. 4. Constants of Diatomic Molecules*; Van Nostrand-Reinhold: New York, 1979.

(27) Brus, L. E.; Bondybey, V. E. *J. Chem. Phys*. **1975**, *63*, 3123.

(28) Bondybey, V. E.; Brus, L. E. *J. Chem. Phys*. **1975**, *63*, 2223.

(29) Lawrence, W. G.; Apkarian, V. A. *J. Chem. Phys*. **1992**, *97*, 2229.

(30) Creuzburg, M.; Wittl, F. *J. Mol. Struct*. **1990**, *222*, 127.

(31) Chergui, M.; Schwentner, N.; Chandrasekharan, V. *J. Chem. Phys*. **1988**, *89*, 1277.

(32) Eloranta, J.; Vaskonen, K.; Häkkänen, H.; Kiljunen, T.; Kunttu, H. *J. Chem. Phys*. **1998**, *109*, 7784.

(33) Pettersson, M.; Lundell, J.; Räsänen, M. *J. Chem. Phys*. **1995**, *103*, 205.

(34) Milligan, D. E.; Jacox, M. E. *J. Chem. Phys* **1969**, *51*, 277.

(35) Jacox, M. E.; Milligan, D. E. *J. Mol. Spectrosc*. **1973**, *48*, 536.

(36) Pettersson, M.; Khriachtchev, L.; Jolkkonen, S.; Lundell, J.; Räsänen, M. Manuscript in preparation.

(37) Pettersson, M.; Lundell, J.; Khriachtchev, L.; Räsänen, M. *J. Chem. Phys*. **1998**, *109*, 618.

(38) Räsänen, M. *J. Mol. Struct*. **1983**, *101*, 275.

(39) Mebel, A. M.; Luna, A.; Lin, M. C.; Morokuma, K. *J. Chem. Phys*. **1996**, *105*, 6439.

(40) Lundell, J. *J. Phys. Chem*. **1995**, *99*, 14290.

(41) Gruebele, M.; Polak, M.; Saykally, R. J. *J. Chem. Phys*. **1987**, *86*, 6631.

(42) Smith, D. F., Jr.; Overend, J.; Decius, J. C.; Gordon, D. J. *J. Chem. Phys*. **1973**, *58*, 1636.

(43) Pak, Y.; Woods, R. C.; Peterson, K. A. *J. Chem. Phys*. **1997**, *106*, 5123.

(44) Bradforth, S. E.; Kim, E. H.; Arnold, D. W.; Neumark, D. M. *J. Chem. Phys*. **1993**, *98*, 800.

(45) Khriachtchev, L.; Pettersson, M.; Isoniemi, E.; Pehkonen, S.; Räsänen, M. *J. Chem. Phys*. **1999**, *111*, 1650.

(46) Persson, B. J.; Roos, B.; Simonson, M. *Chem. Phys. Lett*. **1995**, *234*, 382.

(47) Fajardo, M. E.; Apkarian, V. A. *J. Chem. Phys*. **1988**, *89*, 4102.

(48) Nguyen, M. T.; Sengupta, D.; Vereecken, L.; Peeters, J.; Vanquickenborne, L. G. *J. Phys. Chem*. **1996**, *100*, 1615.

(49) Lundell, J. Private communication.